COMITATO NAZIONALE PER L'ENERGIA NUCLEARE
Laboratori Nazionali di Frascati

LNF - 66/56
15 Novembre 1966

Relazioni presentate al "INTERNATIONAL SYMPOSIUM ON ELECTRON AND POSITRON STORAGE RINGS" - Saclay, September 1966 (PARTE II).

(Nota interna: n. 337)

Servizio Documentazione
dei Laboratori Nazionali di Frascati del CNEN
Casella Postale 70 - Frascati (Roma)

Laboratori Nazionali di Frascati del CNEN
Servizio Documentazione

LNF - 66/56

Nota interna: n. 337
15 Novembre 1966.

RELAZIONI PRESENTATE AL

"INTERNATIONAL SYMPOSIUM ON ELECTRON AND POSITRON STORAGE RINGS" - Saclay, September 1966

PARTE II

1) Project of an experiment on e^+e^- annihilation in two bosons

M. Grilli, V. Manno, M. Nigro, L. Paoluzi, E. Schiavuta, F. Soso, P. Spillantini, V. Valente and R. Visentin.

2) Single boson production in Adone

B. Bartoli, C. Bernardini, F. Felicetti, A. Goggi, D. Scannicchio, V. Silvestrini, F. Vanoli and S. Vitale.

3) Project of an $e^+ + e^- \rightarrow \gamma + \gamma$ or $\pi^o + \gamma$ experiment at Adone

C. Bacci, R. Baldini-Celio, G. Capon, G. P. Murtas, C. Pellegrini, G. Penso, A. Reale, G. Salvini and M. Spinetti.

1) - PROJECT OF AN EXPERIMENT ON $e^+ e^-$ ANNIHILATION IN TWO BOSONS. -

M. Grilli, V. Manno, F. Soso, P. Spillantini, R. Visentin
Laboratori Nazionali di Frascati del C. N. E. N. - Frascati, Roma (Italy)

M. Nigro, E. Schiavuta, V. Valente
Istituto di Fisica dell'Università di Padova

L. Paoluzi
Istituto di Fisica dell'Università di Roma

(Presented by M. Grilli)

We are preparing an experiment on the reactions

(1) $$e^+ e^- = \pi^+ \pi^-$$

(2) $$= K^+ K^-$$

(3) $$= K_1^o K_2^o$$

to be done with Adone.

The reactions (1) and (2) will be studied in the energy range E (total energy of each colliding beam) = 350 ÷ 750 MeV, and the reaction (3) around E = 510 MeV (ϕ resonance).

The theoretical problems connected with such research has been extensively discussed by many authors[1].

Briefly speaking, we can say that some of the more interesting informations, we hope to reach by this experiment, are:

a) the "pole dominance", connected with the ρ and ψ resonance, in the reaction (1) ÷ (3). This concretely corresponds to measuring the relative contributions of the resonant part and of the non-resonant background in these processes;

b) new data on the leptonic decay of these resonances, i. e. on the branching ratios "resonance $\rightarrow e^+ + e^-$. These ratios are, at present, generally measured with a precision not better than 50%;

c) new data on the width of these resonances.

In the following sections we briefly describe the experimental apparatus (§ 1) and the general criteria for the discrimination between the different particles produced (e, μ, π, K) (§ 2). In the third section, we report on the electronic masters we will use for the selection of the reaction (1) and (2) in the different range of energy, excluding the " ψ region" (E = = 507 ÷ 520 MeV), which is separately described in section 4.

1. 1 - Description of the apparatus. -

A general and schematic view of the apparatus is shown in Fig. 1. S_o.. S_c are plastic scintillators, C_{H_2O} is a water Cerenkov counter, C_1.. .. C_6 are spark chambers.

As is discussed with more detail later (§ 1. 2), the counters will be used for an electronic selection between the different channels of the e^+e^- annihilation. This electronic selection will be completed by the observation of the spark chambers.

The Cerenkov counter (n = 1. 33, β_{th} = 0. 75) will discriminate the K from the ($\pi + \mu$ + e) until E = 750 MeV.

C_1 and C_1' (bigap) will be used to measure the collinearity between the two charged products of the e^+e^- annihilation.

The other spark chambers C_2.. C_5 will visualize a large part of the range of the produced particles, to discriminate essentially between π's and μ and electrons.

Details on the counters and spark chambers are summarized in Table I.

Tab. Ia - Dimensions of the counters

Counter	Dimensions (cm^3)
S_o, S_o'	25 x 25 x 0, 1
S_1, S_1'	60 x 60 x 0. 5
S_2, S_2'	90 x 90 x 2
S_K, S_K'	100 x 100 x 2
C_{H_2O}	60 x 60 x 6

Tab. Ib - Some details of the spark chambers

Sp. ch.	Dimensions (cm^2)	Plates no	Plates Thickness (mm)	Plates Gap (mm)	Material
C_o	48 x 48	21	0. 25	8. 5	Al(1. 42 g/cm^2)
$C_1(C_1')^{(x)}$	50 x 50	--	----	2x75	-----
C_2	87 x 87	6	3. 0	8	Fe
(C_2', C_3, C_3')		1	1, 5		(15, 2 g/cm^2)
$C_4^{(*)}(C_4')$	100x105	--	----	7-10	
$C_5^{(*)}(C_5')$	125x130	--	----	7-10	

(x) - Bigap

(*) - C_4 and C_5 are made up by 11 single monogaps with variable absorbers (Fe) between these monogaps.

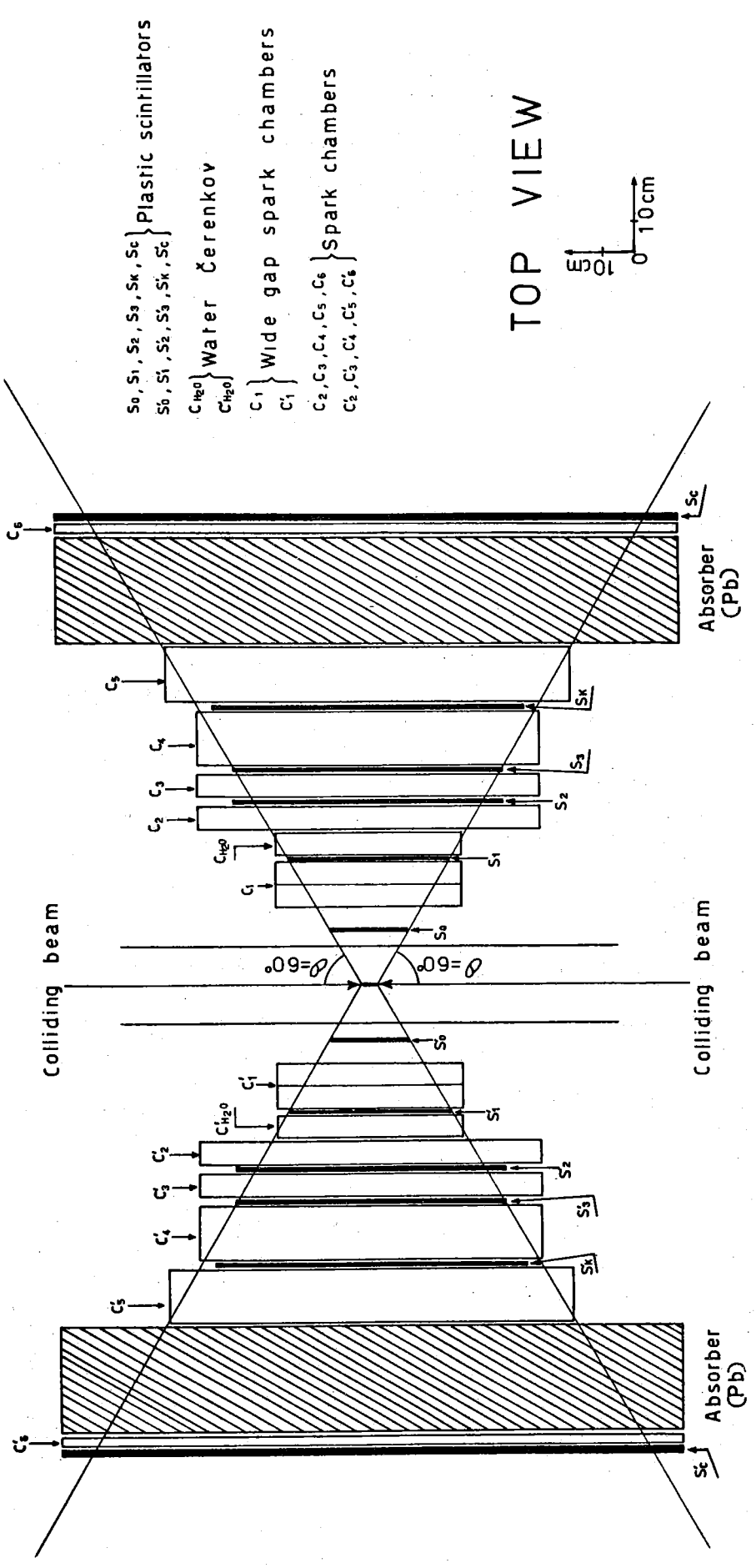

FIG. 1 - Schematic design of the apparatus for the experiment

The angular range covered by our apparatus is $\Delta\theta$ (zenith) = $= \Delta\varphi$ (azimuth) = $60^{o} \div 120^{o}$, corresponding to about 2,5 sr (taking into account the $\text{sen}^2\theta$ dependence of the production cross section in the case of a two boson annihilation). The median plane of the apparatus coincides with the machine's plane. The angles θ and φ are specified in Fig. 2.

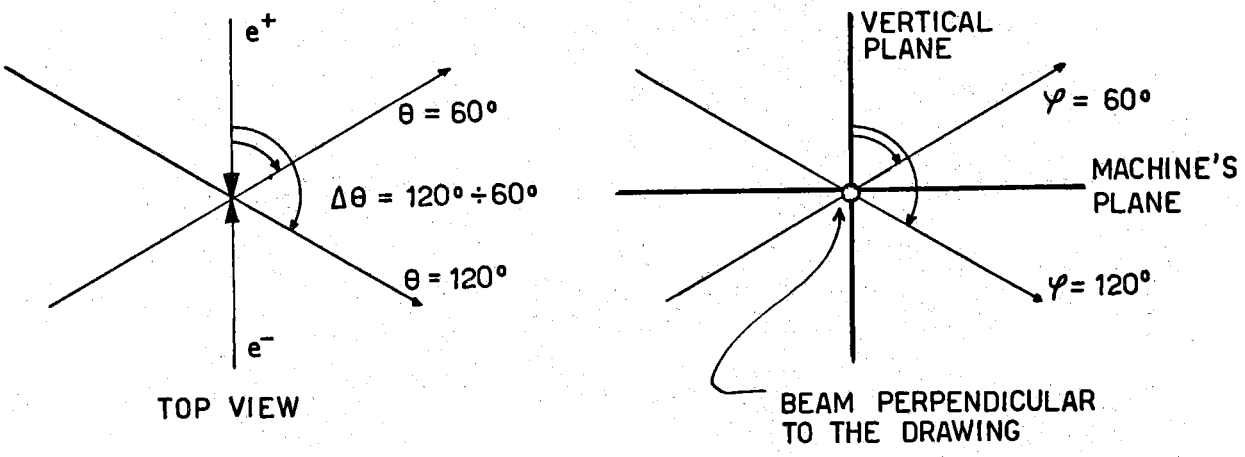

FIG. 2 - Angular range covered by the apparatus.

The counting rates, expected for reactions (1) and (2) with our apparatus, are summarized in Table II. In making these previsions we have used the cross sections calculated by Gatto et al., the value of luminosity reported in the table and we have included the losses due to the decay in flight of slow K, to the nuclear interaction of pions etc.....

1.2 - Discrimination between the different particles produced. -

We discuss now the criteria to follow in order to discriminate between the different particles produced in a two body annihilation e^+e^-.

First, in order to select the two body against the many body-annihilations, we will require a collinearity (into $\pm\ 0,5^{o}$) between the two charged products.

Table II - Events for hour for reaction (1) and (2), expected in our experiment.

E	400	510	750
$L(cm^{-2}h^{-1})$	$0,25.10^{33}$	$0,3.10^{33}$	$0,5.10^{33}$
$\pi^+\pi^-$	50	3	1
K^+K^-	--	150	0.5

Moreover we will require for a "good event", that the charged products come from the intersecting region between the two colliding beams.

1.2.1 - We begin now by discussing the criteria to be used against the cosmic rays.

We will have about 13.000 cosmic rays/h, passing through our telescope. From

these counts only 5% are in time with the beam's collision (resolving time = $= \pm 2.5$ ns), which means 650 counts/h.

Moreover, we have in our master trigger an anticoincidence against the cosmic rays:

$$(4) \qquad \overline{(RC)} = \overline{(FS_1S_1'S_2'S_c')} \text{ or } \overline{(FS_1'S_1S_2S_c)}$$

(F = timing pulse from the machine).

With a 1% inefficiency of this anticoincidence(x), due to a 10% inefficiency of the large counters (1 x 1 m^2) S_c or S_c' for a minimum ionizing particle, we have 6,5 counts/h.

Table III

Reaction	Master	E
$\pi^+\pi^-$	(a) $FS_1S_1'S_2S_2'\,\overline{RC}$	350 - 500 MeV
	(b) $FS_1S_1'S_2S_2'$ (C or C')$(\overline{S_3 \text{ or } S_3'})^3\overline{RC}$	500 - 750 MeV
K^+K^-	(c) $FS_oS_o'S_1S_1'(\overline{S_3C})(\overline{S_3'C'})(\overline{CC'})\overline{RC}$	520 - 640 MeV
	(d) $FS_1S_1'S_2S_2'(\overline{CC'})\overline{RC}$(trigger for spark chambers)	640 - 750 MeV
	(e) $FS_1S_1'S_2S_2'\overline{CC'}(S_K \text{ or } S_K')\,\overline{RC}$ (trigger for scaler)	640 - 750 MeV

This counting rate is reduced by other peculiar requirements imposed in the selection of the different particles (see § 2,2 and Table III) and finally is reduced by at least a factor 1/1000 by the scanning of the photos of the spark chamber. This last factor is largely due to the requirement to come from the interaction region, imposed for a "good event".

We are reconsidering all the problem in the sense that we are thinking how to reduce, in the electronic preselection, the counting rate due to the cosmic rays.

1.2.2 - We will discuss now the general criteria we will use to discriminate between the different particles produced in a two-body e^+e^- annihilation.

(x) - This estimate is optimistic as we assume that no cosmic rays would be lost for a nuclear or electromagnetic interaction in passing through our telescope from S_c to S_c', or vice versa.

(i) the $e/(\pi+\mu)$ discrimination will be made by means of the e. m. showers produced by the electrons. For E > 500 MeV, we will also operate an electronic preselection against the electrons by means of a "shower counter", formed by the two spark chamber. C_1 and C_2 (total thickness = 2 r. l.) and the scintillation counters S_2 and S_3.

The $e/(\pi+\mu)$ discrimination will be completed by observing the tracks of the particles in the spark chambers $C_1 .. C_5$. The total thickness of the these chambers is equivalent to about 8 r. l.

(ii) $K/(\pi+\mu+ e)$ - In the case of K, we must consider two completely different regions:

a) φ region (E = 507 ÷ 520 MeV).

The produced K is very slow, so we have a short range and, conversely, a high energy loss in the counters. So in the K's selection we will put a cutoff in the pulse height of the trigger counters. Moreover, if necessary, we could also add a condition on the different time of flight between the slow K's and a relativistic particle (π, μ, e). In our case this difference is of the order of 4 ns.

b) E = 520 - 750 MeV.

The K's are always below the threshold of the water Cerenkov C_{H_2O}, and have a definite range.

Unfortunately, owing to the presence of the charged secondary of K's decay or capture, it is not possible to impose separately the two conditions, i. e. veto condition on the Cerenkov counter and on the S_3 counter (see Table IIIc)).

Also the electronic preselection of the K's will be tested and completed by looking, at the photos, to the range of produced K's. In fact, on the available data on the nuclear interactions of the K, we estimated that until E = 750 MeV, more than 75% of the produced K will reach the end of it's range without suffering a nuclear interaction.

We will take advantage of this situation also in the electronic selection of the K^+K^- reaction (see Table III (e)) by requiring a pulse height larger than a given threshold in a counter (S_K or S'_K) placed near the end of the range of the K.

(iii) The π/μ discrimination is based on the clear difference between these two particles with respect to the nuclear interactions.

As a consequence of this fact in our apparatus only 1% of π against a 85% of μ will reach the more external counters S_c or S'_c. The thickness X_π of the material we need between the source and these counters S_c (or S'_c) in order to stop 99% of produced pions as a function of the energy E is given in Fig. 3. The value of X_π has been evaluated by means of the present available measurements of nuclear interactions of pions.

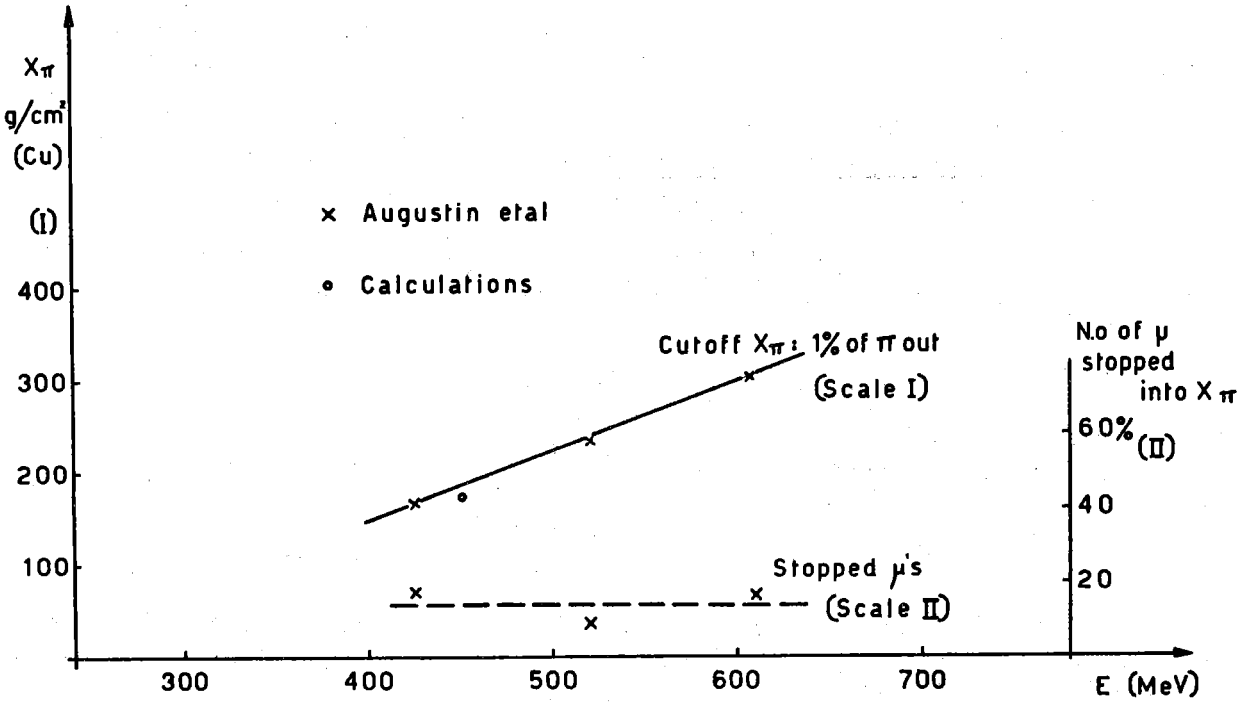

FIG. 3 - Thickness X_π of the absorber (Cu), as a function of the energy E. The absorber X_π stop 99% of pions. X_π has been evaluated by the present available measurements on the nuclear interaction of pions.

The electronic preselection between π and μ will be accurately completed by the scanning of the photos of the $C_1 .. C_5$ spark chambers. In this regard, we note that the fraction of $\pi^+\pi^-$ pairs with at least one pion interacting in the $C_1 .. C_5$ s. ch., ranges from 100% to 90% (E = 350 - 750 MeV).

The "external" s. ch. C_6 (or C_6') is placed to control the efficiency of counter S_c (or S_c'), for the particles which come out from the absorber X_π.

1.3 - Master for reaction (1) and (2) (no φ region).

Starting from the general criteria described before we have chosen for the different reactions to be studied the masters reported in Table III.

We would like to add few comments to this table:

(i) - the region E = 500 MeV (φ region) will be discussed separately (see § 1.4) for the reactions K^+K^- and $K_1^0K_2^0$.

(ii) - The differences between the masters used in the different energy ranges come from simple physical reasons. For example, we must change the K^+K^- master at E = 640 MeV, because for this energy the K reach the veto counter S_3 (or S_3').

(III) - The basic trigger is given by a fast 5-fold coincidence ($FS_1S_1'S_2S_2'$) between two counters from each part of the telescope with a timing pulse (F) coming from Adone.

We have about 2 cm of F_e between S_1 and S_2. On the basis of the measurements on the background made by the ACO and Stanford Groups, we hope that this situation makes a good working condition.

(IV) - The losses on the counting rate due to different reasons nuclear interaction, decay of slow K, counter's inefficiency etc.) are summarized in Table IV.

Table IV - Losses on the counting rate

Reaction	Fractional loss	
$\pi^+\pi^-$	10 + 15%	E = 350 - 750 MeV
K^+K^-	60 + 20%	E = 520 - 750 MeV

The losses are due, essentially, to the nuclear interaction before reaching the master's counter or to the decay in flight in the cases of $\pi^+\pi^-$ and K^+K^-, respectively.

These losses can be evaluated with enough accuracy in such a way to result in an incertitude on the real counting rate, which is certainly less than 5%.

(V) - The contamination on the counting rate $\pi^+\pi^-$ and K^+K^-, due to the other particles produced in a e^+e^- annihilation, is reported in Table V. The only serious contamination is due to electrons pairs as we expect $(e^+e^-)/(K^+K^-) \sim$ ~ 100 $(e^+e^-)/(\pi^+\pi^-) \sim 40$, for E = 550 - 750 MeV.

Table V - Contaminations expected on "$\pi^+\pi^-$" and "K^+K^-" events (see tect).

Reaction	Energy range	Fractional contamination
$\pi^+\pi^-$	500-750 MeV	5% of produced electrons (~0, 1%) 2% of produced μ's (~0, 1%) 10% of produced K's (~1%)
K^+K^-	520-750 MeV	2 + 0.5% of produced electrons (~0.1%) 3 + 1% " " pions (~1%) 1% " " μ (~0.1%)

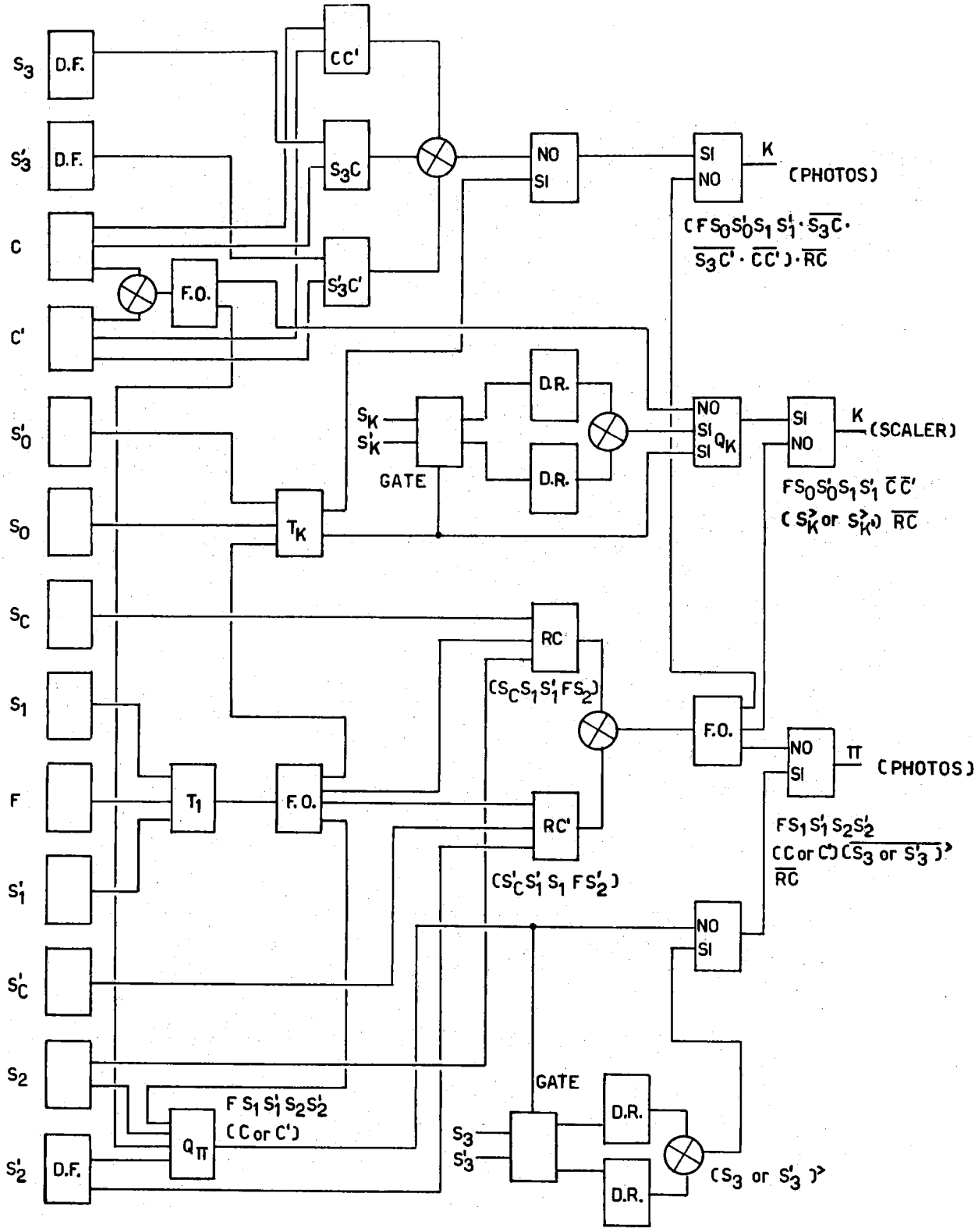

FIG. 4 - Block diagram of the electronics.

In any case, after the scanning of s. ch. photos, the residual contamination (in parenthesis in Table V) are only a small percentage of the good events.

The block diagram of the electronics to be used is reported in Fig. 4.

1. 4 - Master for reaction (2) and (3) in the " φ region" (E = 507 - 520 MeV).

1. 4. 1 - K^+K^- - Starting from the general criteria explained in § 1. 2. 2 we will use for the K^+K^- pairs a trigger:

(5) $$FS_0^{>}S_0^{'>}S_1^{'>}(\overline{RC})$$

This trigger corresponds to a pair of charged particles, not due to cosmic ray, in time with the beam's collision and with pulse heights clearly larger (at least a factor 5) than those due to relativistic particles in the counters $S_0S_0'S_1'$.

To measure the reaction (2) in the " φ region" we will make some change in our telescope, as sketched in Fig. 5.

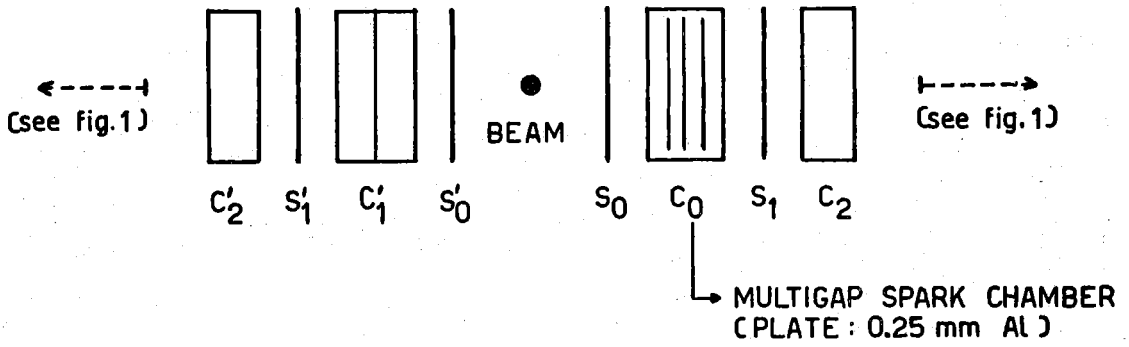

FIG. 5 - Experimental apparatus for the reaction $e^+e^- \longrightarrow K^+K^-$, in the " φ region". C_0 is a multigap spark chamber (thickness of single plate: 0. 25 mm Al). The other counters and spark chambers are as indicated in Fig. 1.

The two K's stop, respectively, in S_1' and in the multiplate spark chamber C_0. The range resolution ($\Delta R/R = \pm 7\%$) of K's in this chamber (thickness of a single plate: 0,25 mm Al) corresponds to a resolution in the energy E of the colliding beams $\Delta E = \pm 0.5$ MeV.

We have extimated that, owing to the strong conditions we imposed in the K selection (5), the contaminations due to different particles are negligible.

1. 4. 2 - $K_1^oK_2^o$ - We will observe the reaction (3) in the φ region looking to the decay

(6) $$K_1^o \rightarrow \pi^+ + \pi^-$$

We will take advantage of the following facts:

(I) - owing the small value of the velocity of the K^o ($\beta \sim 0.25$) the two decay pions are about collinear. The angle between the two tracks is less than 40^o.

(II) - Owing to the short life time of K_o (~ 0.1 ns) this particle decays inside 1 cm from the production point.

(III) - A large part of the decay pions ($\sim 60\%$) will stop without suffering a nuclear interaction ($T_\pi = 60 \div 170$ MeV).

The trigger to select (6) will be the same as for the collinear pairs $\pi^+\pi^-$.

The geometrical efficiency of our apparatus in looking the decay (6) is estimated to be $\sim 10\%$.

REFERENCES. -

(1) - See, for example: R. Gatto, Proceedings of the International Symposium on Electron and Photon Interaction at High Energies, Hamburg, 1965, vol. I, pag. 106; N. Cabibbo and R. Gatto, Phys. Rev. 124, 1577 (1961).

2) - SINGLE BOSON PRODUCTION IN ADONE.

B. Bartoli, C. Bernardini, F. Felicetti, V. Silvestrini
Laboratori Nazionali di Frascati del CNEN - Roma (Italy)

A. Goggi, D. Scannicchio
Istituto di Fisica dell'Università, Pavia and Istituto Nazionale di Fisica Nucleare, Sezione di Pavia.

F. Vanoli, S. Vitale
Istituto di Fisica Superiore dell'Università, Napoli and Istituto Nazionale di Fisica Nucleare, Sezione di Napoli.

2. 1 - Statement of the problem. -

Neutral non strange bosons can be singly produced in e^+e^- collisions; in particular they will be produced at rest in e^+e^- storage rings. The production cross section is peaked around the boson mass and reproduces, as a function of the total center of mass energy of the primaries, the line shape characteristic of a free unstable particle[1]. Thus, a plot of the counting rate versus total c. m. energy of the colliding e^+e^- should exhibit a line structure over a flat non resonant background: a storage ring can be used in this sense as a boson mass spectrometer.

Actually, quantum numbers conservation imposes some limitations on the intensity of the boson lines. Production to the lowest electromagnetic order (one photon channel) is allowed only when the final boson has $J^{PC} = 1^{--}$. When $J^{PC} = 1^{++}$, 2^{++} the line intensity will be depressed by a factor $e^4 \approx 10^{-4}$; other cases will be even more severely contrasted by helicity arguments[1].

2. 2 - The φ^o case. -

A typical feature of single boson production in e^+e^- storage rings is the absence of strongly interacting partners to the produced particle.

The φ^o case is particularly interesting in that φ^o's life time is so short that when it is strongly produced it also usually decays in presence of strong fields.

High energy forward photoproduction of φ^o on nuclei[2] shows some perplexing features suggesting a possible difference in the line shape of a free φ^o from that usually observed. This remark suggests that an accurate investigation of the ρ^o production in Adone be made.

2.3 - Adone as a boson mass spectrometer. -

The mass range of Adone as a mass spectrometer goes up to 3 BeV, twice the maximum energy of each primary electron.

The lower mass limit at which the ring can be safely operated is not well known: it presumably extends down to 600 MeV without any trouble and a non negligible luminosity[3].

The mass resolution is given by the energy spread of the primaries. The total c. m. energy definition should be given to within a few hundred keV according to the design characteristics of the machine[3]. In view of the present knowledge on the line width of strongly decaying bosons this figure for the energy spread should be largely adequate. A line narrower than, say, 500 keV will have its width masked and its peak intensity reduced by averaging over the energy spread of the beam particles.

2.4 - The experimental setup. -

The non resonant background of e^+e^- reactions will span the same variety as the boson decay products. However a large fraction of non resonant events will be due to electron-positron scattering whereas electron-positron boson decay should be rare. It could be convenient to consider the possibility of reducing e^+e^- counting rates but this seems at present not so easy to achieve all over the wide energy range to be scanned. In any case e^+e^- scattering simulates only a boson decaying into two charged particles.

A simple detection system accepting both charged products and γ rays is shown in Fig. 1. No attempt has been made to distin guish among charged particles in this system; however pulse height analysis could be of help in some cases.

The accepted solid angle of the counter system in Fig. 1 is 60% of the total.

Fig. 1 shows 4 scintillation counter sandwiches, numbered from 1 to 4; counters in each sandwich are labeled A, B, C moving from the interaction region of the primary beams (at the center of the array).

Lead converters are inserted in between counters A, B and B; C.

A charged particle reaching sandwich n^o 1, say, will at least give a pulse in A; this event will be classified as 1_c and corresponds to A or A + B or A + B + C. A + C will possibly be electronically excluded.

A γ ray will usually not give a pulse in A (less than 10%, depending on the angle, will convert into the 1 mm steel walls of the donut; in this case the γ ray will be classified as a charged particle). Shower production in the lead converters can be detected by pulses in B or C or both

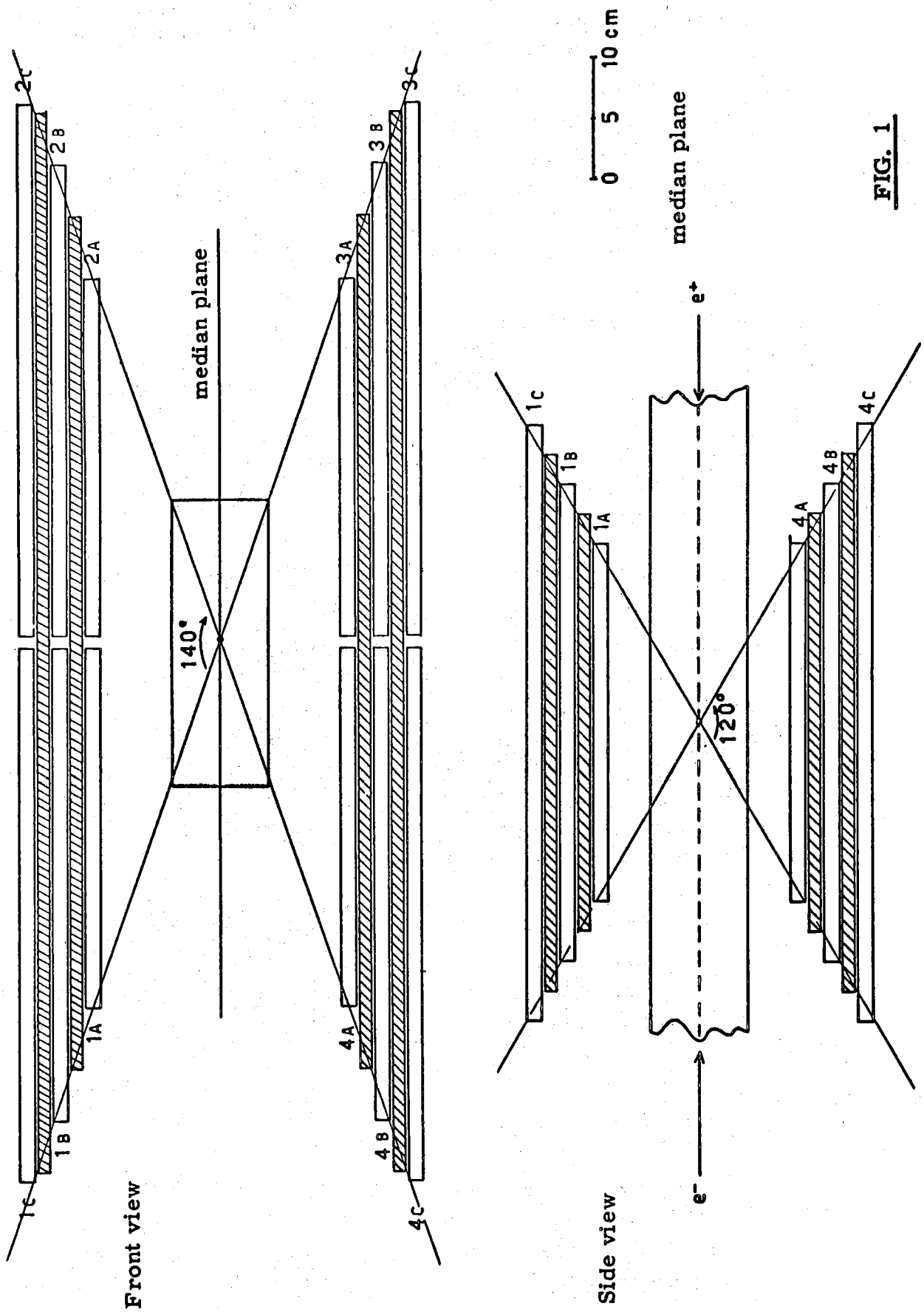
Front view
median plane
140°
1c
1B
1A
2A
2B
2c
3A
3B
3c
4A
4B
4c
Side view
median plane
e⁻
e⁺
120°
0 5 10 cm

FIG. 1

(B + C) in anticoincidence with A. The conversion efficiency can be made high enough by choosing each lead converter 1.5 radiation lengths thick: this corresponds to about 95% conversion efficiency.

Events like $\overline{A} + B$ or $\overline{A} + C$ or $\overline{A} + B + C$ will be classified as neutrals; thus 1_N means a neutral triggering sandwich n° 1.

In the following, by the symbol 1 we will mean either an event 1_N or 1_C and a similar notation will be used for the other channels. We will further classify events as follows:

a) two or more body decay events correspond to such coincidences as 1 + 3 or 2 + 4;

b) three or more body decay events correspond to coincidences 1 + 2, 2 + 3, 3 + 4, 4 + 1, 1 + 2 + 3, 1 + 2 + 4, 1 + 3 + 4, 2 + 3 + 4;

c) four or more body decay events correspond to coincidences 1 + 2 + 3 + 4.

It must be noted that the possible outcomes are ordered according to increasing smallest number of decay products in each group (a, b, c). The groups actually overlap.

2.5 - A fast method to explore the whole mass range. -

The main idea is that of exploring the whole mass range by continuously varying the energy of the ring from the minimum to the maximum. A slow triangular modulation of the machine field appears easily feasible provided the period is longer than one minute[4].

The main virtue of this method is that intense single boson lines will be simultaneously evident after a short running time wherever they are in the scanned mass range. Smaller bumps will gain statistical significance as the time goes on: there one has to decide when to stop according to the fluctuations of the non resonant background.

A crude sketch of the expected plot (actually of the cross section versus energy) is given in Fig. 2 including only the known vector bosons ρ^o, ω^o, ϕ^o.

Once a bump is observed the energy modulation can be restricted to the neighborhood of the relevant energy to obtain better statistics in a short time.

2.6 - Counting rate estimates. -

Let us call ΔE the amplitude of the energy modulation; ΔE will be divided in $\mathcal{N}$ channels, $\delta E = \Delta E/\mathcal{N}$ wide each.

The channel width can be at minimum of the order of the energy spread of the primary electrons: we will fix $\delta E = 1$ MeV as a typical figu

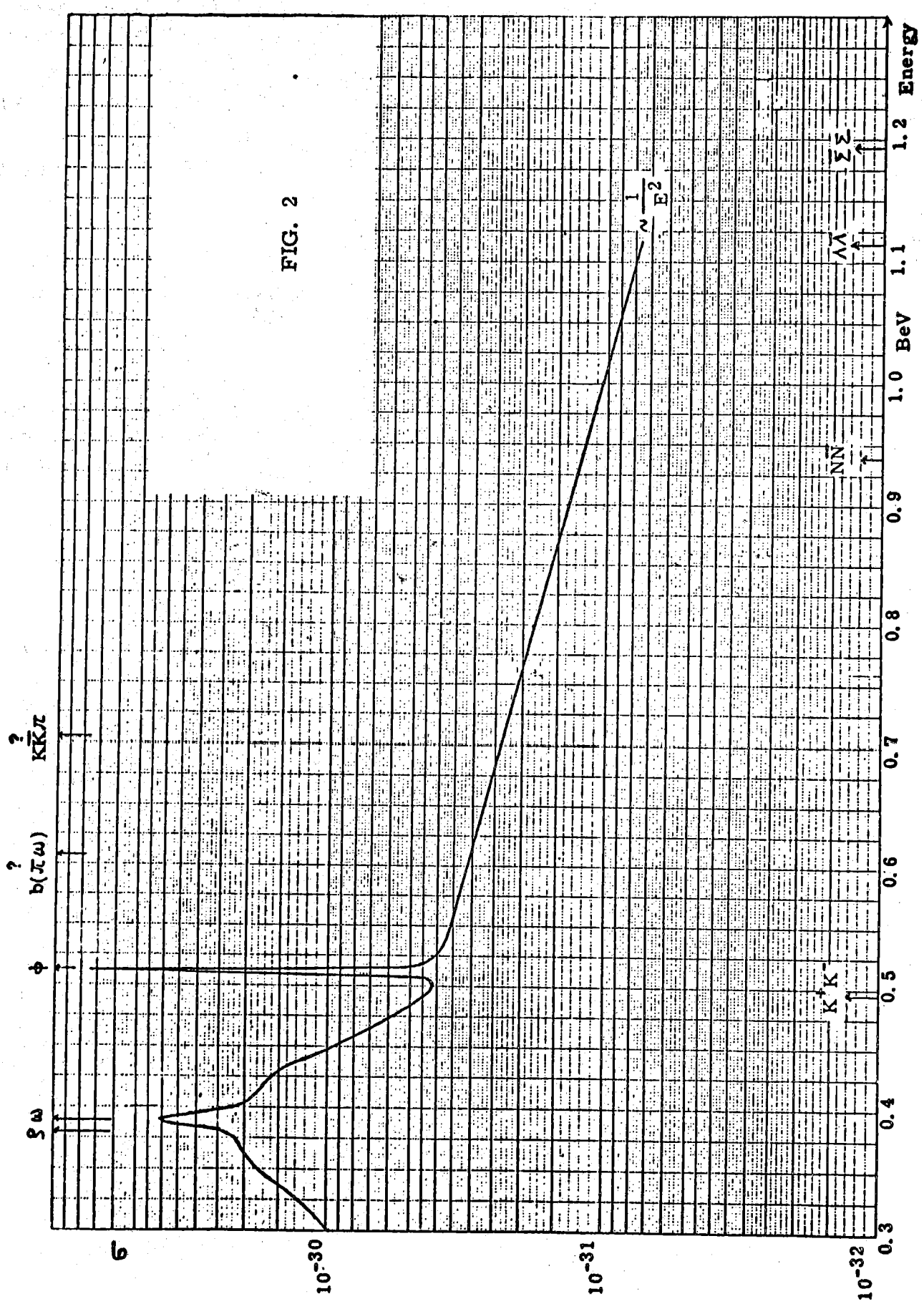
σ
10^{-30}
10^{-31}
10^{-32}
0.3
0.4
0.5
0.6
0.7
0.8
0.9
1.0 BeV
1.1
1.2 Energy
ρω
φ
? b(πω)
? KK̄π
K^+K^-
$N\bar{N}$
$\Lambda\bar{\Lambda}$
$\Sigma\bar{\Sigma}$
$\sim \frac{1}{E^2}$

FIG. 2

re. $\mathcal{N}^{-1}$ measures the fraction of the total time spent on each channel, since triangular modulation of the energy provides a simple linear time-energy correspondence.

Assuming modulation over the full energy range, that is $\Delta E \simeq$ $\simeq$ 1000 MeV, we will have a typical duty-cycle of 10^{-3} per MeV.

The number of counts per channel after a total running time t is given by

$$n_c = \frac{1}{\mathcal{N}} L \sigma t$$

where L is the luminosity and σ is the cross section of any detectable event. σ can be divided in three parts:

σ_r = cross section for resonant processes
σ_{nr} = cross section for non resonant processes from the interaction region.
σ_b = equivalent cross section for machine background (coincidence events from the gas or the walls, equivalent cross section for accidentals).

By taking

$$\mathcal{N} = 10^3; \quad t = 100 \text{ hrs}; \quad L = 5 \times 10^{32} \text{ cm}^{-2} \text{ hr}^{-1}$$

it follows that

$$n_c = 5 \times 10^{31} \sigma \text{ (in cm}^2\text{) events/channel}$$

2.7 - First comment on background. -

Both σ_{nr} and σ_b are supposed to be flat over several 10 MeV. However σ_{nr} can exhibit some curvature when the energy passes through the threshold of a pair production process; σ_b can simulate a peaking behaviour because of systematic machine failure at some energy. In the first case (σ_{nr}) we just say that pair thresholds are known, otherwise they are interesting in themselves. In the second case (σ_b) a dummy counter system not illuminated by the good source can monitor the unwanted background alone (it must be noted in this occasion that the strict time-position correspondence for machine background events makes every point near the interaction region equivalent).

To the number of counts n_c one must add an uniform contribution n' from cosmic rays.

Non resonant events are unavoidable (a part from a possible reduction of the contribution of e^+e^- scattering); machine background and cosmic rays can be minimized and we shall present later the expected situation.

2.8 - Criterion for the evidence of a peak. -

A Monte Carlo simulation of the experiment is in progress in order to investigate the criteria for the most convenient use of machine time.

An example of this study is shown in Fig. 3(x). The aim of this program is that of

a) indicating when the full range scanning has to be abandoned and a closer investigation around a particular mass value has to be initiated;
b) giving a rule for rejection of "optical illusions" produced by fluctuations.

Unfortunately, these considerations are model dependent and will be probably modified after the experiment initiates.

2.9 - Backgrounds. -

a) We shall consider first non resonant background. As we already remarked in par. 2.4, the main beam-beam contribution simulating a boson decaying into two charged bodies is due to e^+e^- scattering

$$\sigma_{nr} \simeq \varepsilon_e \sigma_{scatt}.$$

where ε_e is a rejection factor for electrons and σ_{scatt} is the e^+e^- scattering cross section integrated over the detected solid angle.

We do not know yet whether electrons can be rejected with a good efficiency or not; for the moment being ε_e will be left unspecified.

To evaluate σ_{scatt} we use the formula

$$\frac{d\sigma}{d\Omega} = \frac{5 \times 10^{-26}}{\gamma^2} \frac{(1+\frac{1}{3}\cos^2\theta)^2}{(1-\cos\theta)^2} \text{ cm}^2$$

where γ is the electron energy in mass units and θ the scattering angle.

Integration over the apparatus gives with a very good approximation

$$\sigma_{scatt} = \frac{5 \times 10^{-26}}{\gamma^2} \frac{\Delta\Omega}{\sin^2\theta_{min}}$$

where $\Delta\Omega$ is the total detected solid angle; θ_{min} is the minimum θ value of the scattered electrons. With $\Delta\Omega = 0.7 \times 4\pi$ and $\theta_{min} = 30^o$ as in Fig. 1 we get

---

(x) - We are grateful to Mr. B. Coluzzi for the preparation of this material.

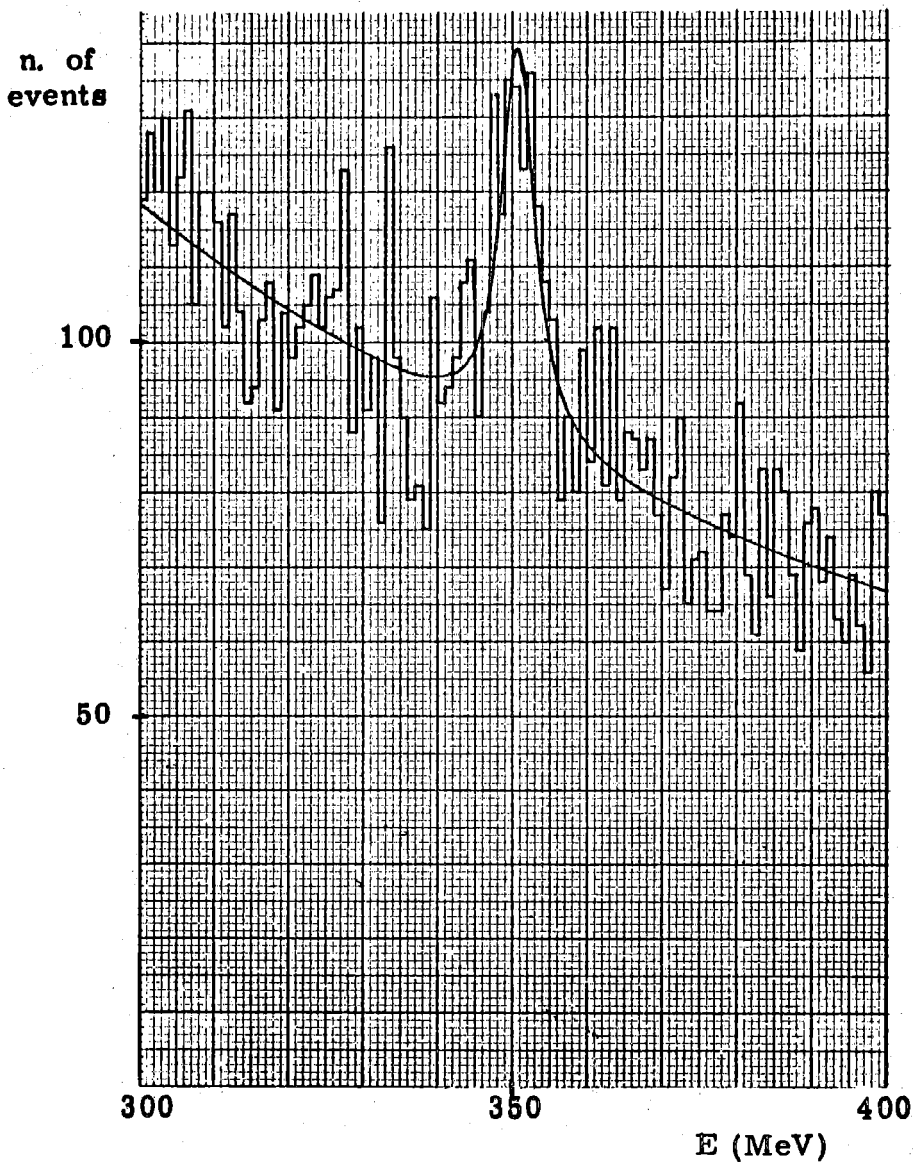

	Input	Scanning	
M_R	700	701.5	MeV
h. w.	5	5.4	MeV
n_{peak}	60	52.3	
peak area	437	449.5	

$$n_{bckgrd}(E_R) = 90$$

χ^2 (non resonant) = 197.5 (99 d. of fr.)

χ^2 (resonant) = 108 (96 d. of fr.)

FIG. 3

$$\sigma_{scatt} \cong \frac{1.8 \times 10^{-24}}{\gamma^2} \text{ cm}^2$$

Thus σ_{scatt} goes from 5×10^{-30} cm^2 at E = 300 MeV to 2×10^{-31} cm^2 at E = 1.5 BeV. Note that going from $\theta_{min} = 30^o$ to $\theta_{min} = 45^o$ σ_{scatt} will be reduced by a factor 2.4; at the same time $\Delta\Omega$ is only reduced by a factor 0.8. Smaller counters than in Fig. 1 could prove convenient if a rejection factor ε_e appreciably less than 1 could not be obtained.

b) Machine background constitutes the central headache. Of the 4×10^{11} particles circulating at full intensity (sum of the two beams), nearly 2×10^7 are lost per second (precise values depend slowly on the energy). Assuming an uniform loss all around the ring and taking into account the geometry of the machine a figure of 10^{-2} is expected for the fraction of the total source lenght seen by the counters in Fig. 1.

Thus a flux of 2×10^5 particles per second constitutes the machine background.

Showers generated in the donut will invest the counters laterally and must be quite efficiently shielded. Expected rates are as follows

2-fold coinc. accidentals: $10^4\ \varepsilon^2$ per second
true 2-fold coincidences: $10^5\ \varepsilon^2\ p_2$ per second

Here ε is a shielding factor; p_2 is the probability that 2 or more particles generated by the same lost beam particle are detected in coincidence.

Clearly ε must be less than 1/300 in order that the equivalent cross section σ_b be substantially less than 10^{-30} cm^2 (see par. 2.6). Recent background measurements with ACO at Orsay and with the Princeton-Stanford rings seem to indicate that machine background can be reduced to the desired low level.

c) Cosmic rays would give a uniform in time counting rate of 10^5 particles per hr if not properly shielded. A substantial reduction can be achieved however by requiring a time coincidence of the events with the passage of a bunch in the interaction region. This coincidence (already used in the more difficult case of AdA[5]) will provide a duty cycle factor of 5×10^{-2} thus reducing the cosmic ray events to 5×10^3/hr.

An anticoincidence roof will further reject cosmic rays and we hope that this anticoincidence will be able to reduce the cosmic rays rate to less than 50/hr.

REFERENCES. -

(1) - R. Gatto, Theoretical aspects of colliding beam experiments; in Ergebnisse der Exacten Naturwissenschaften vol. 39, 106 (1965).
(2) - B. B. Blumenthal et al., Phys. Rev. Letters 15, 210 (1965); We one the remark in this par. to the review presented by G. Salvini at the 1965 Accelerator Conference at Frascati.
(3) - F. Amman, Dimensioni dei fasci, vite medie, luminosità e caratteristiche della zona di interazione in Adone, Laboratori Nazionali di Frascati, Internal Report LNF - 66/6 (1966).
(4) - F. Amman, private communication.
(5) - C. Bernardini et al., Nuovo Cimento 34, 1473 (1964).

3) - PROJECT OF AN $e^+ + e^- \rightarrow \gamma + \gamma$ OR $\pi^\circ + \gamma$ EXPERIMENT AT ADONE. -

C. Bacci, G. Penso, G. Salvini
Istituto di Fisica dell'Università, Roma; and INFN Sezione di Roma

G. Capon, G. P. Murtas, C. Pellegrini, A. Reale, M. Spinetti
Laboratori Nazionali di Frascati del CNEN, Roma (Italy)

R. Baldini-Celio
Borsista CNR.

Introduction. -

We have planned an experimental apparatus to detect the two reactions

(1) $$e^+ + e^- \rightarrow \gamma + \gamma$$

(2) $$e^+ + e^- \rightarrow \pi^\circ + \gamma$$

in the electron positron storage ring Adone.

Reactions (1) and (2) in the Born approximation are described by the following diagrams

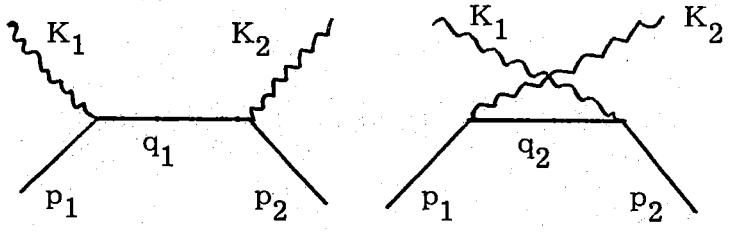

for reaction (1)

where $q_1^2 = 4E^2 \operatorname{sen}^2\theta/2$; $q_2^2 = 4E^2 \cos^2\theta/2$

and

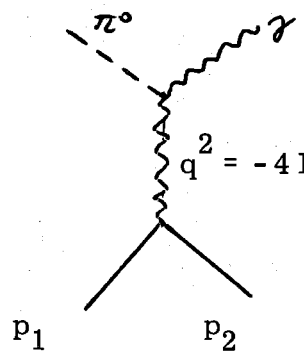

for reaction (2)

θ is the angle between the line of flight of the two photons and the e^+e^- direction; 2E the total C. M. energy.

Briefly we discuss first the reasons for measuring process (1).

a) Verification of electrodinamics (e. d.) for space like values of the momentum of the virtual electron, in a momentum interval between 0. 26 and 2. 9 GeV.

This is of particular interest also in connection with some recent measurement at Cambridge(1), Cornell(2), Hamburg(3) on the reaction

$$\gamma + \text{nucleus} \rightarrow \text{nucleus} + e^+ + e^-.$$

b) In the process (1) the propagator is a virtual electron not signifi cally affected by deviations due to the vector mesons, like ρ, ω, φ as the photon propagator in some others reactions,like

$$e^+ + e^- \rightarrow e^+ + e^-$$
$$e^+ + e^- \rightarrow \mu^+ + \mu^-$$

c) From an experimental point of view an important feature of reac tion (1) is that it allows a chek of e. d. by measuring angular distribution at different energies of e^+e^-.

This is a great advantage, if one consider the difficulty of having, at last in a first stage, a monitoring system with a few percent accuracy.

Point c) is not true for the process (2). A measurement of the cross section is then strictly connected to the measurement of reaction (1) from the point of view of the experimental apparatus and also for monitoring request.

Process (2) is an important tool for studying vector bosons: coupling constants between γ, ρ, ω and φ, mixing angle ω-φ and it is also a possible method for detecting new vector bosons.

In fact the cross section of process (2) can be relatively high when the total energy 2E approach the mass of the vector bosons (ρ, ω, φ), then strongly decrease to about 10^{-35} cm^2 when 2E is far from the energy of these resonances.

Experimental apparatus. -

The experimental apparatus for detection of the $\gamma\gamma$ and $\pi^0\gamma$ reac tions is drawn in Fig. 1 and 2.

It consists of 4 spark chambers at 90^o to the electron beam and two others s. c. at small angles, that we call for convenience "Monitor Cham bers" (M. C.).

The first chambers are used to measure the angular distribution between 45^o and 135^o degrees,while the M. C.,are used to measure the cross section at θ 25^o.

Scintillation counter system gives the right trigger when there are

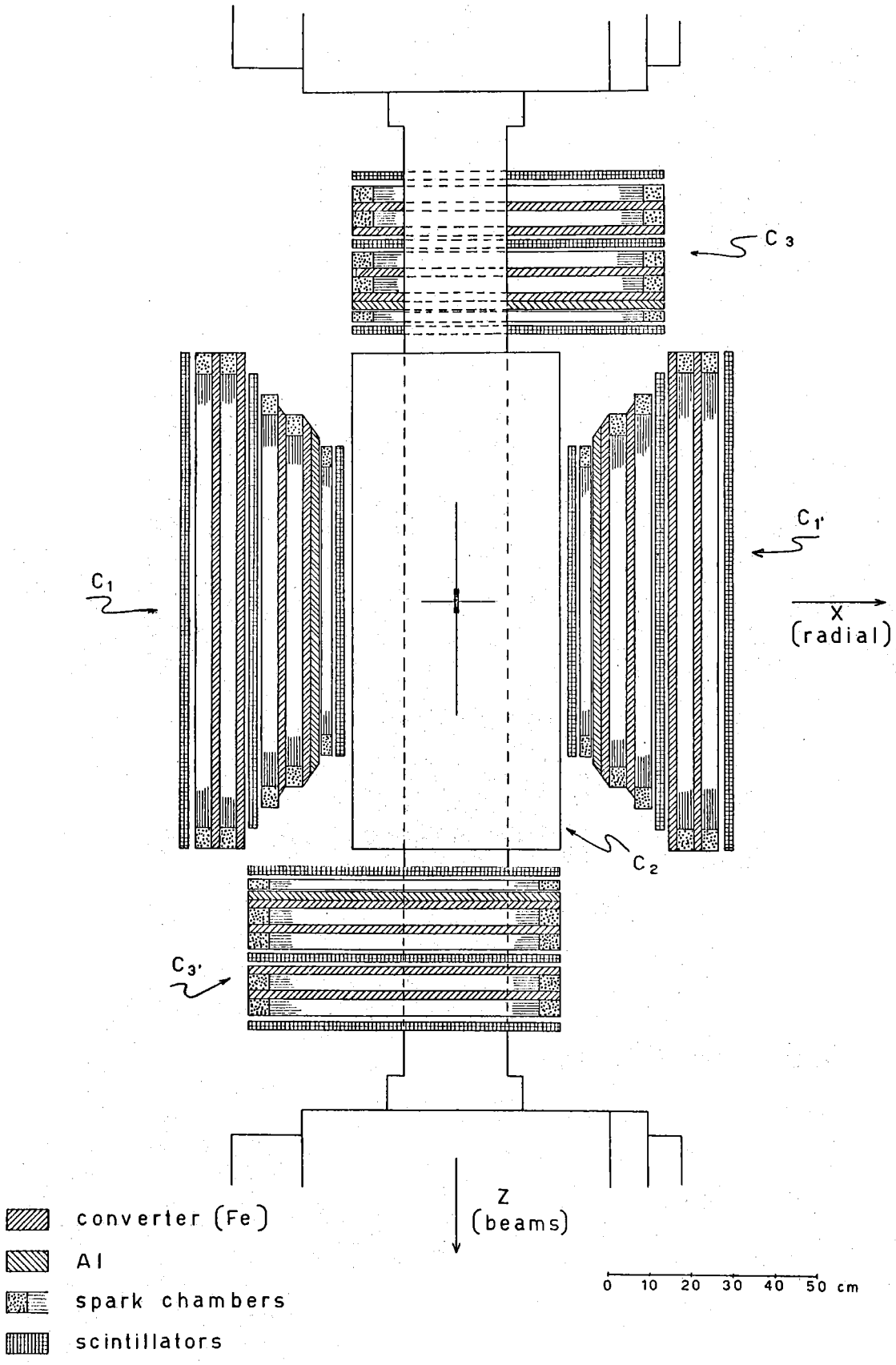
C 3
C 1'
C 1
X
(radial)
C 2
C 3'
Z
(beams)
converter (Fe)
Al
spark chambers
scintillators
0 10 20 30 40 50 cm

FIG. 1

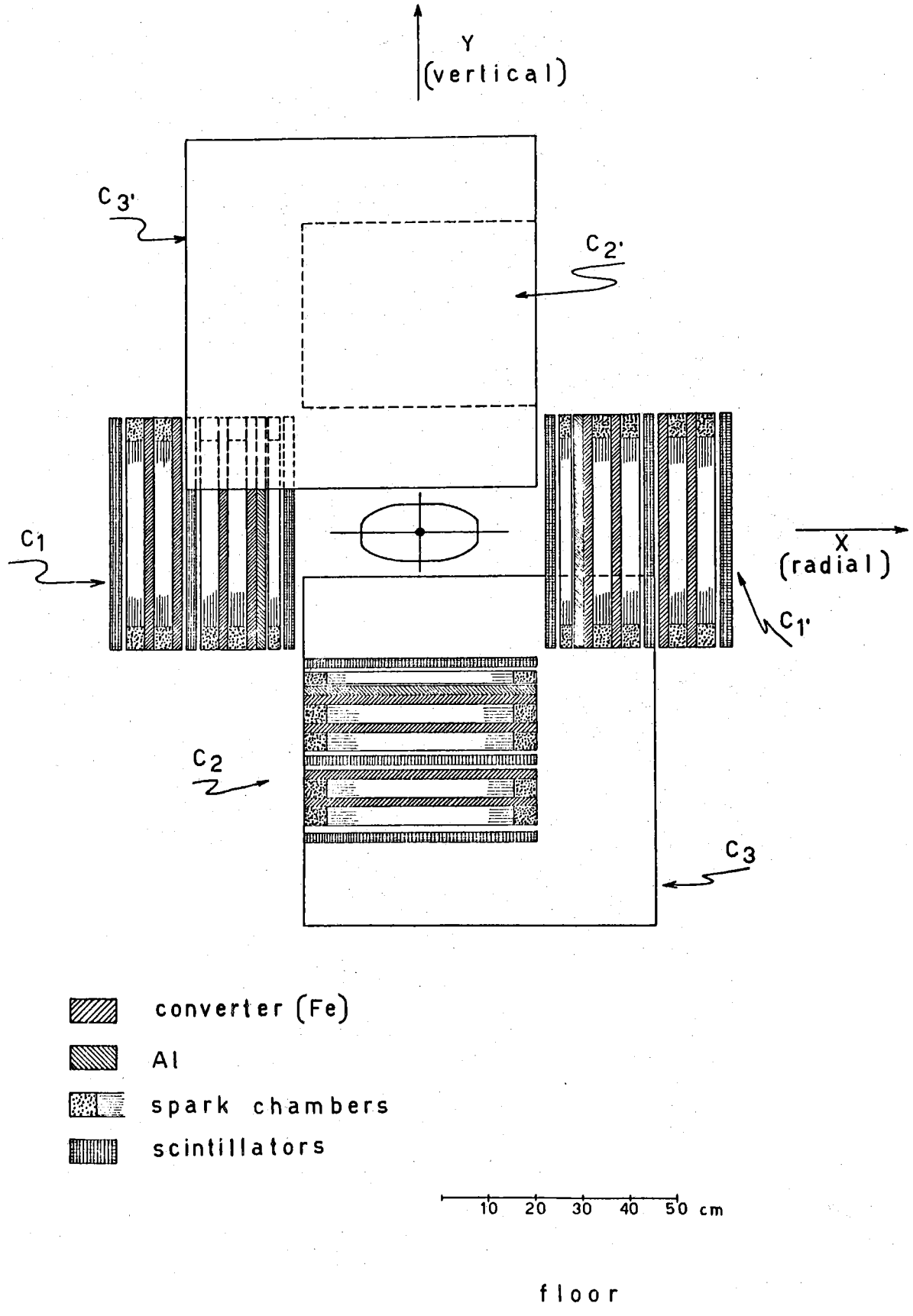
Y
(vertical)
C3'
C2'
C1
X
(radial)
C1'
C2
C3
converter (Fe)
Al
spark chambers
scintillators
10 20 30 40 50 cm
floor

FIG. 2

almost two photons without any changed particle. The solid angle covered by the system is

	4 x 1.07 sr	for the 90° Chambers
and	2 x 0.39 sr	for the M. C.

The system is modular so that one could start to measure with a very simple structure and use afterwards a more complete set up.

We may reconstruct the direction of the photons to a few degrees accuracy by observing the development of the shower.

Actually we have done some measurement with different types of chambers (wide-gap and multigaps chamber 10 cm thick) looking to the electrons after 1-2 radiation lenghts of converter and we obtain, f. i., the direction of 500 MeV photons with $\pm 1,5 \div 2$ degree of accuracy.

Analysis of reaction (1) and (2). -

The cross section $d\sigma/(d\cos\theta)$ for (1) is given[4] in Fig. 3.

We can see that the angular distribution can also be written in the following way:

$$Y(\theta) = \left| F(q_1^2) \right|^2 + \left| F(q_2^2) \right|^2 \cdot tg^4 \theta/2$$

(see Fig. 4), where $F(q^2)$ is the form factor which is comprehensive of the vertices and the electron propagators.

An approximate way of writing the form factor can be[4]

$$F(q^2) = (1 + \frac{q^2}{Q^2})^{-1}$$

where Q is the breakdown parameter.

If the q. e. is valid in our energy region the ratio $Y(\theta)/Y(25^\circ)$ must be independent from the energy. If Q is finite, these ratio must change with the energy.(v. fig. 5).

The cross section[4] for $e^+ + e^- \rightarrow \pi^\circ + \gamma$ is plotted in Fig. 6.

$\sigma(E)$ rises up to 10^{-31} cm^2 only when the C. M. energy is equal of the mass of the mesons ρ, ω, φ.

Reactions (1) and (2) are observed simultaneously in the experimental set up.

Two photons coming from reaction (1) are aligned (apart from the effect of radiative corrections), while photons coming from reaction (2) will exibit a typical angular correlation and in this way we think to separate the

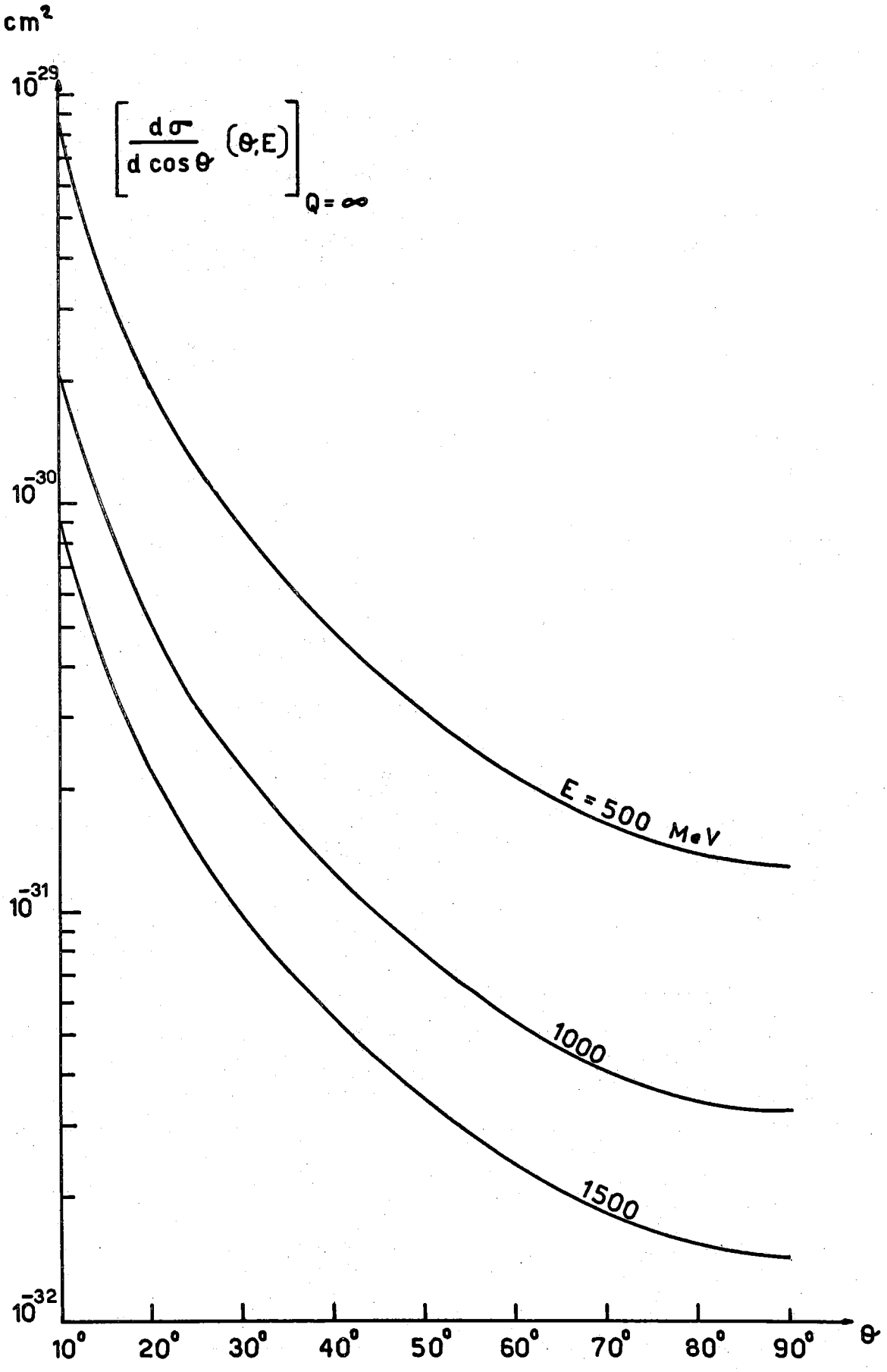
cm²
10⁻²⁹
10⁻³⁰
10⁻³¹
10⁻³²
[dσ/d cos θ (θ;E)]Q=∞
E = 500 MeV
1000
1500
10°
20°
30°
40°
50°
60°
70°
80°
90°
θ

FIG. 3

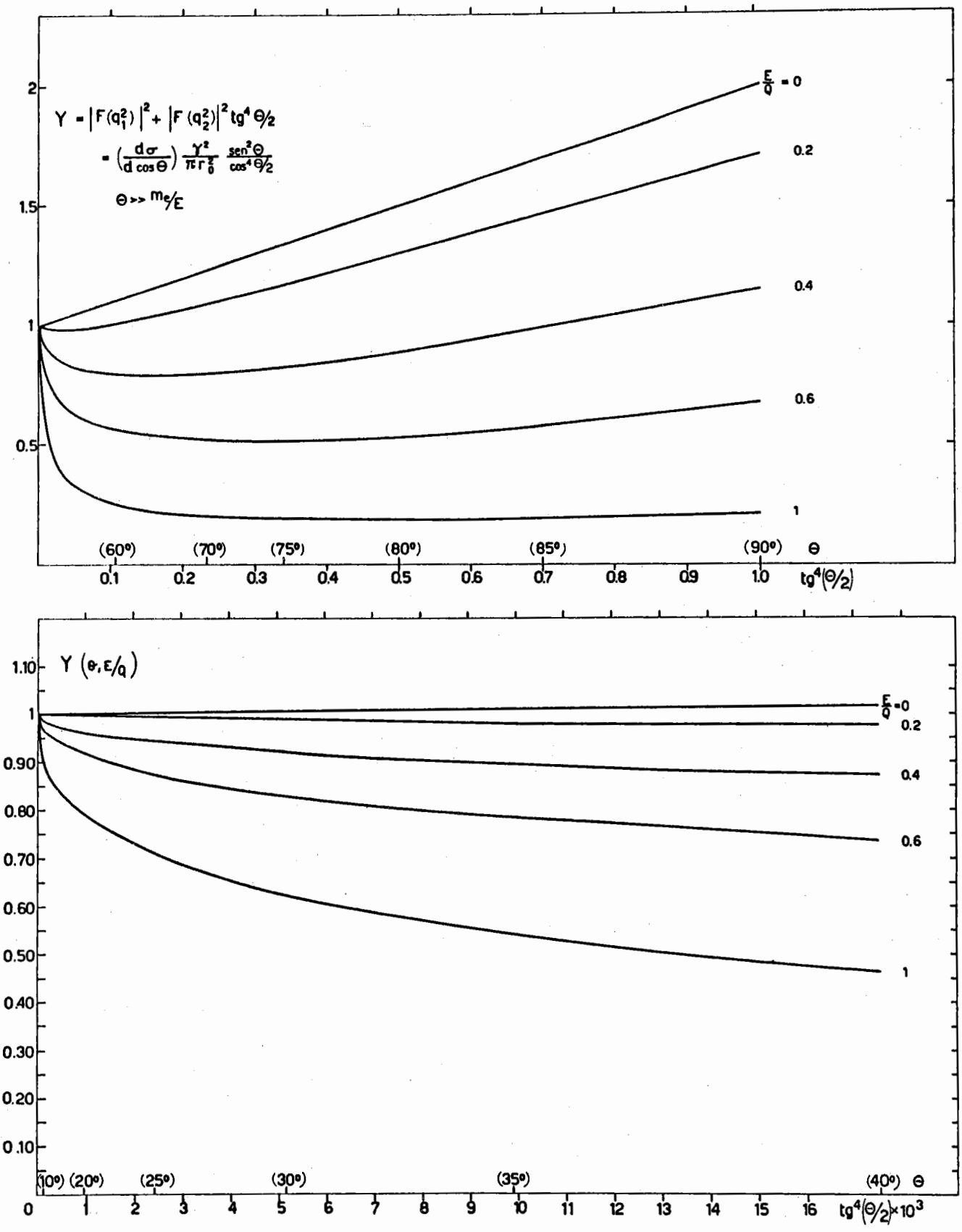
$Y = |F(q_1^2)|^2 + |F(q_2^2)|^2 \operatorname{tg}^4 \Theta/2$
$= \left(\frac{d\sigma}{d\cos\Theta}\right) \frac{\gamma^2}{\pi r_0^2} \frac{\operatorname{sen}^2\Theta}{\cos^4\Theta/2}$
$\Theta >> m_e/E$
E/Q = 0
0.2
0.4
0.6
1
(60°) (70°) (75°) (80°) (85°) (90°) Θ
0.1 0.2 0.3 0.4 0.5 0.6 0.7 0.8 0.9 1.0 $\operatorname{tg}^4(\Theta/2)$
$Y(\theta, E/Q)$
E/Q = 0
0.2
0.4
0.6
1
(10°) (20°) (25°) (30°) (35°) (40°) Θ
0 1 2 3 4 5 6 7 8 9 10 11 12 13 14 15 16 $\operatorname{tg}^4(\Theta/2) \times 10^3$

FIG. 4

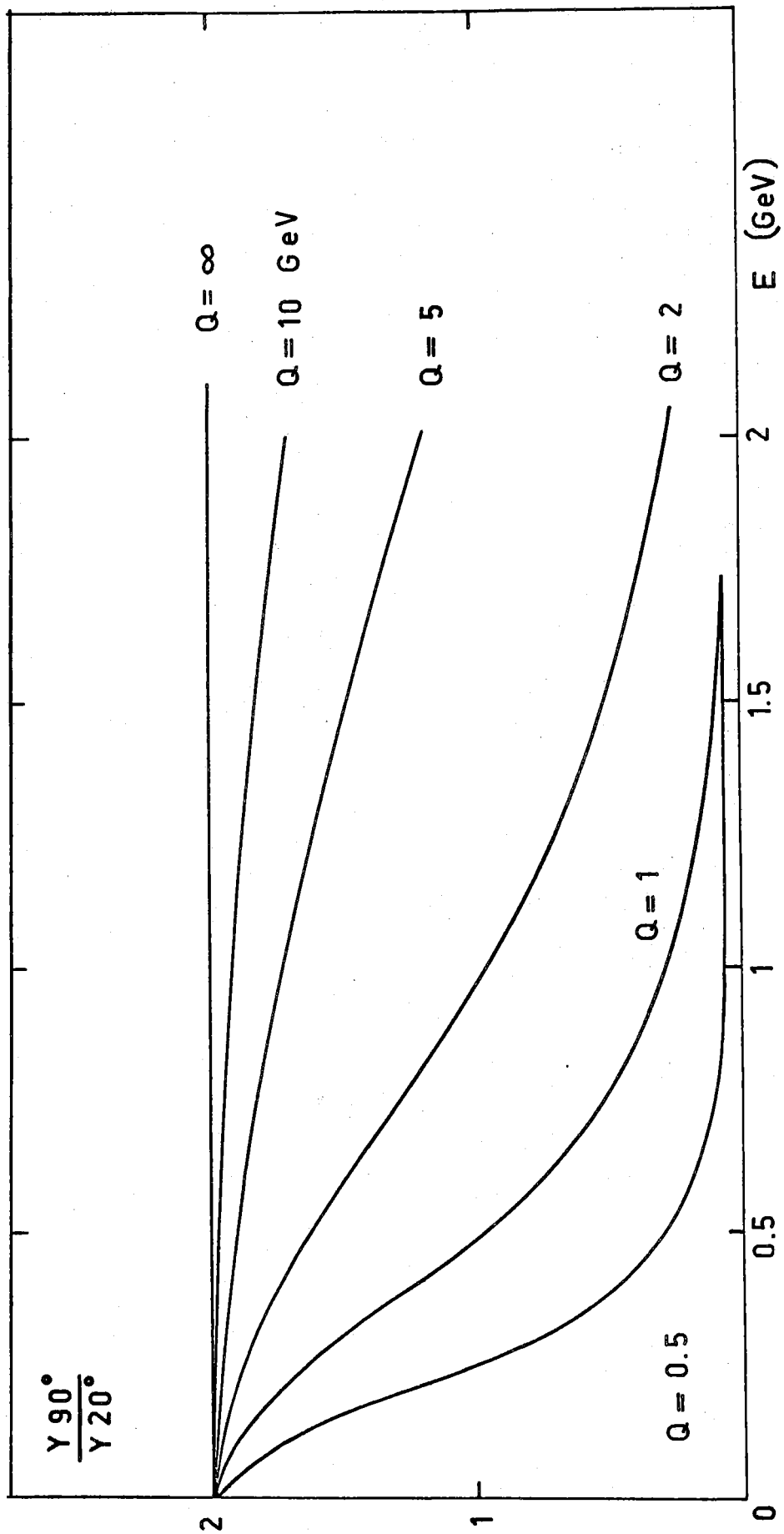

FIG. 5

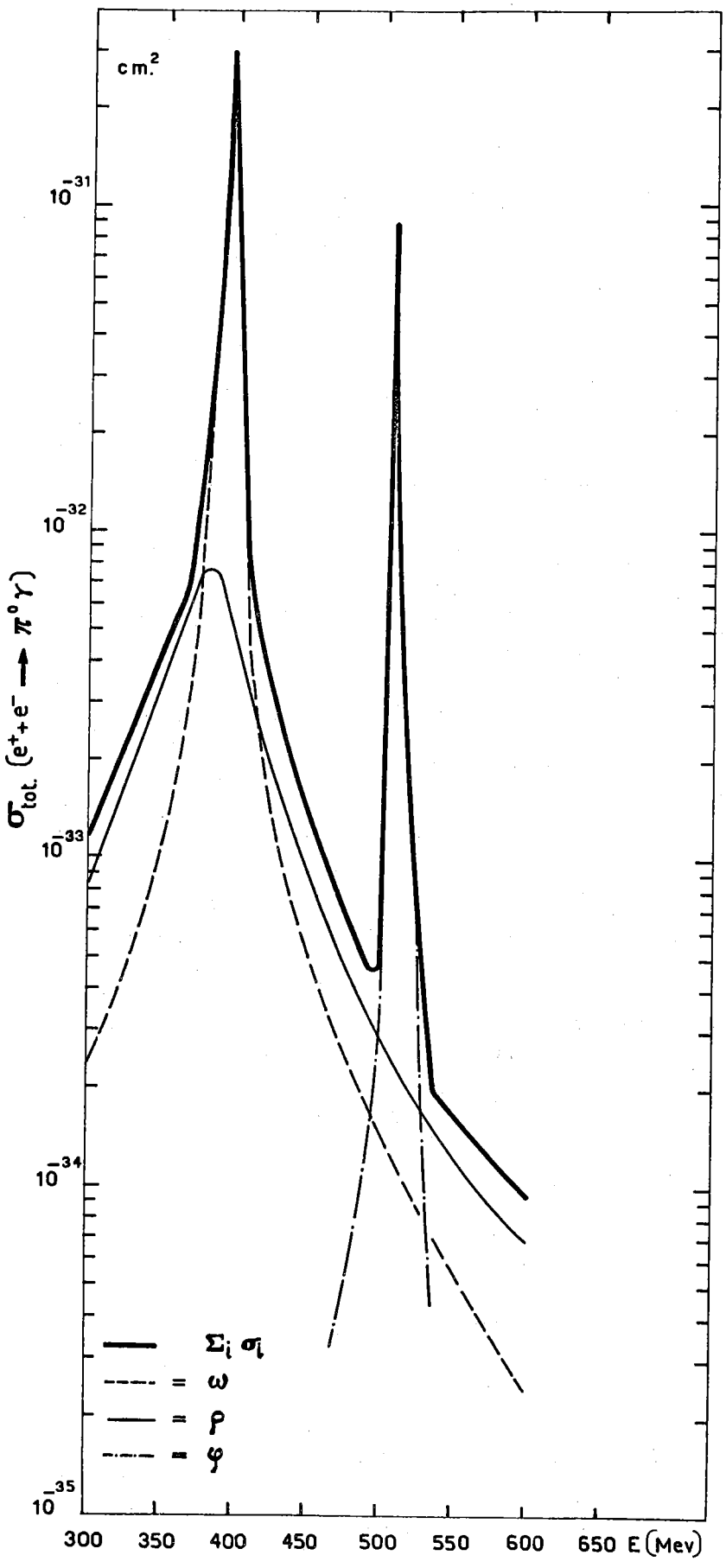
cm.²
10⁻³¹
10⁻³²
10⁻³³
10⁻³⁴
10⁻³⁵
σtot. (e⁺+e⁻ → π⁰γ)
Σi σi
= ω
= ρ
= φ
300
350
400
450
500
550
600
650 E (Mev)

FIG. 6

two processes.

Radiative corrections. -

In comparing the angular distribution at different energies we must take in account the radiative corrections, which depend, as well known, from the angular acceptance $2\Delta\theta$ of experimental set up.

In our case we can choose $\Delta\theta$ a posteriori because we use spark chambers as detectors.

For each $\Delta\theta$ value one has a given δ and a certain background of events due to other processes. One has then the possibility of choosen the $\Delta\theta$ value which gives a minimum value of δ and a maximum rejection against unwanted events. On the other hand by varying $\Delta\theta$ it is possible to make a check on the evaluation of the radiative corrections.

TABLE I

θ	θ	E = 500 MeV	1000	1500
20^o	$2,5^o$	δ =-0,056	δ =-0,06	δ = - 0,064
	5^o	δ =-0,019	δ =-0,02	δ = - 0,022
90^o	$2,5^o$	δ =-0,114	δ =-0,12	δ = - 0,131
	5^o	δ =- 0,065	δ =-0,07	δ = - 0,075

In table I we report some values of the radiative corrections δ [5] for different electron energies and for different angular acceptances.

Radiactive corrections for the process (2) are probably negligible because the measurement is done in poor geometry.

Counting rates. -

Assuming a machine luminosity

$$L = \frac{10^{33}}{1.5} E\ (GeV) \qquad (cm^2 hours)^{-1}$$

the counting rates for the 90^o chambers are report in Fig. 7.

For the monitor chambers the rates are about half of these values.

Quoting only statistical errors in the rates, in table II we report in

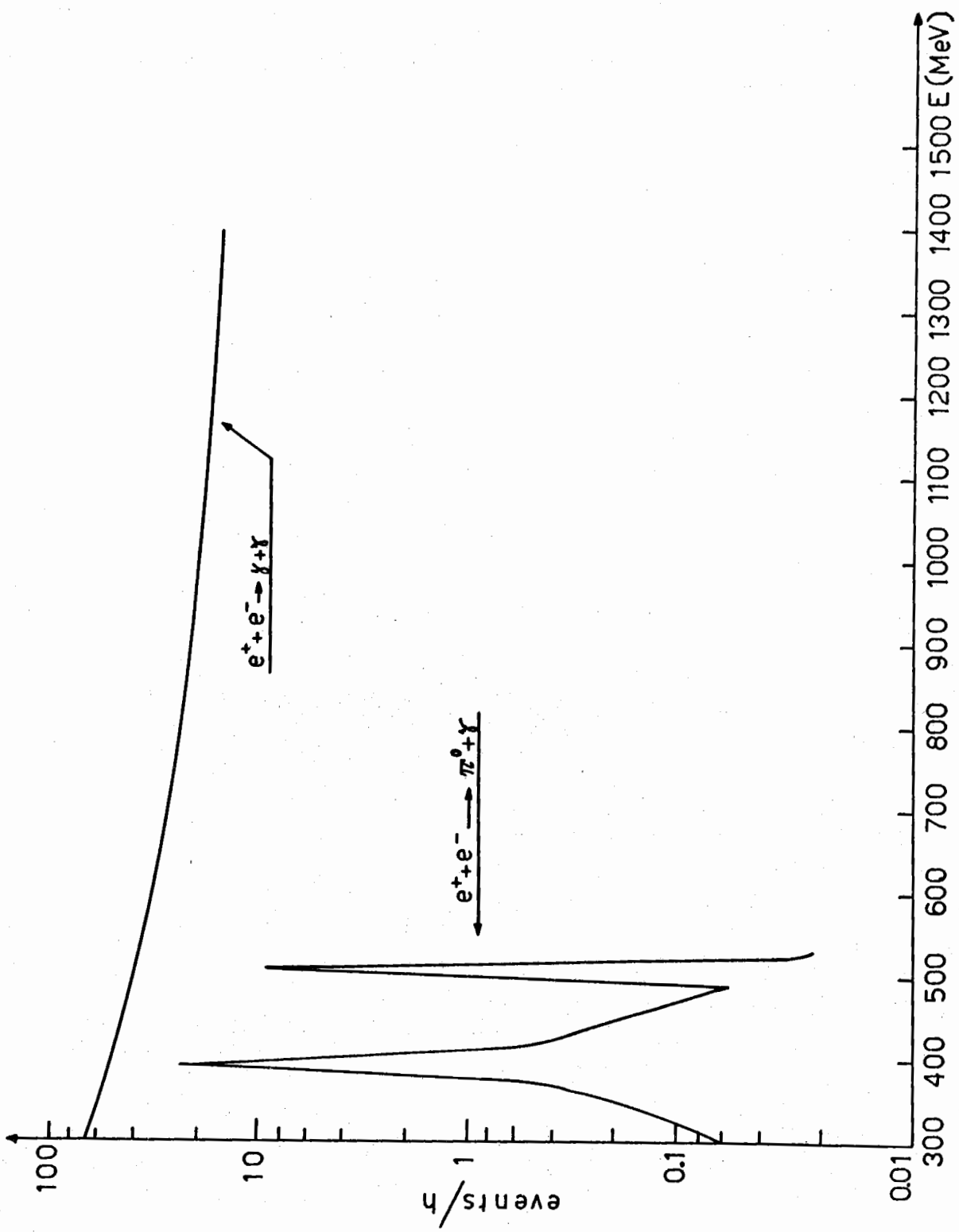
100
10
1
0.1
0.01
events/h
300 400 500 600 700 800 900 1000 1100 1200 1300 1400 1500 E(MeV)
e⁺+e⁻→γ+γ
e⁺+e⁻ ⟶ π⁰+γ

FIG. 7

first column the measurement time we need to geet, at a machine energy of 1.5 GeV, the number of events reported in column 2 corresponding to a precision on R reported in column 3. The numbers refer to an angular range in θ of $\pm 5^{o}$ around 85^{o}. The contribution of the others intervals centered around different values of θ is of the some order of magnitude. In column 4 are reported the lower limits on the breakdown parameter Q one can get on the basis of the precision obtained in the measurement of R.

TABLE II

time hours	events	$(\Delta R/R)\%$	Q GeV
35	100	10	9
140	400	5	13
3500	10000	1	28

Background. -

One could also present the ratio between experimental and theoretical value of R as a function of the momentum transfer q.

At 90^{o} $q_1^2 = q_2^2 = 2E^2$ and we can best the values of R for q ranging between 0.5 and 2.12 GeV with a precision going from 3 to 5% in a measuring time, for each point, of 140 hours.

For what concernes the background we estimated that there are no processes which can simulate seriously the 2γ annihilation if a suitable thickness is used for the wall of the doughnut in the beam crossing point.

The background due to showers from diffused electrons or photons can be probably ruled out in scanning the pictures.

REFERENCES. -

(1) - R. B. Blumenthal et al., Phys. Rev. 144, 1199 (1966).
(2) - J. Asbury et al., Desy-Columbia wide angle pair production experiments, Presented at the Conference on High Energy Nuclear Physics, Berkeley (sett. 1966).
(3) - E. Eisenhandler et al., Bull. Am. Phys. Soc. 11, 20 (1966).
(4) - R. Gatto, Proceedings of the International Symposium on Electron and Photon Interaction at High Energies, Hamburg (June 1965), vol. I, pag. 106.
(5) - Y. S. Tsay, Phys. Rev. 137, 730 (1965).